ISIJ International, Vol. 42 (2002), No. 1, pp. 100–105

Evolution of Microstructure and Texture Associated with Ridging in Ferritic Stainless Steels

SooHo PARK, KwangYuk KIM, YongDeuk LEE and ChanGyung PARK[1)]

Stainless Steel Research Group, Technical Research Laboratories, Pohang Iron and Steel Co., Ltd., Pohang, 790-785 Korea. E-mail: soohopark@posco.co.kr 1) Department of Materials Science and Engineering, Pohang University of Science and Technology, Pohang, 790-784 Korea.

(*Received on September 12, 2001; accepted in final form on September 27, 2001*)

The evolution of microstructure and texture in two ferritic stainless steels was investigated in order to identify the existence of grain colonies associated with ridging and their origin. Special attentions were placed upon examining how the columnar crystals with an initial [001]//ND orientation in continuously-cast slabs can affect the formation of the grain colonies or band structures in the cold-rolled sheet specimens. The rolling and recrystallization textures at each process stage were examined by the orientation distribution function (ODF). Micro-texture measurements using an electron back-scattered diffraction (EBSD) technique were carried out on the ND, RD, and TD section, respectively. The existence of grain colonies having both {001}⟨110⟩ and {112}⟨110⟩ orientations at the central region of the sheets was clearly identified. These orientations were caused by both the crystal rotation toward α-fibre texture, which is stable orientation during rolling and the suppressed recrystallization. The relation between the presence of grain colonies and ridging phenomena was discussed.

KEY WORDS: microtexture; ridging; grain colony; EBSD; stainless steel.

1. Introduction

The 'ridging' phenomenon is one of the serious problems observed on the surface of sheet-type ferritic stainless steels, which are deformed by plastic forming processes, such as cold-rolling and deep-drawing. It has been suggested that the ridging is caused by anisotropic plastic flow of a material operated by the alternating mixed bands of crystallographic textures.[1–3)] However, the suggestion has not been proved yet because of the absence of technique to detect the spatial distribution of the texture components after revealed as grain clusters or bands. Recently, electron back-scattered diffraction (EBSD) analysis has been emerged as a pertinent means of providing spatial distribution of micro-texture in a high spatial resolution.[4,5)] Even using this technique, the presence of grain colonies or clusters proposed in the theoretical models has not been identified.[6–8)]

The aim of present study is to identify the grain colonies associated with ridging by investigating the evolution of microstructure and texture in ferritic stainless steels. The investigation has been extended from the as-cast state to the cold-rolled and final annealed condition by using EBSD and ODF analyses. Especially, our primary interest was focused on whether grain colonies are present or not in finally annealed sheets. Special attentions were also placed upon examining how the columnar crystals in continuously-cast slabs can affect the formation of the grain colonies or band structures in the cold-rolled sheet specimens.

2. Experimental

The materials studied in the current study were continuously cast type 430 and 409L stainless steels. The chemical composition of the steels is shown in **Table 1**. The columnar zone of the continuously cast slab was cut in the form of a bar (200W×150L×25T (mm)) as shown in **Fig. 1**. The initial orientation of columnar crystals was identified as $\{001\}\langle uvw\rangle$. The microstructure of 409L steel was fully ferritic phase while 430 steel contains about 35% of the austenite phase with ferrite matrix. After a homogenization heat-treatment, the bars were reduced from 25 mm to 3.5 mm in thickness by hot rolling followed by annealing. The plates were, then, cold-rolled with 80% thickness reduction, followed by final annealing. The annealing condition is shown in **Table 2**. Microstructural and texture analyses were made at the end of each process, denoted as slab, hot-rolled (HR), hot-rolled & annealed (HRA), cold-rolled (CR), and cold-rolled & annealed (CRA).

Microstructural observations and crystallographic orientation measurements were made on the ND, RD and TD planes of the steels as shown in Fig.1. The orientation image microscopy (OIM) system installed in a Philips XL-

Table 1. Chemical composition of two ferritic stainless steels (wt%).

	C	Si	Mn	Cr	Ti	N	γ(%)
409L	0.008	0.56	0.25	11.4	0.23	0.009	0
430	0.048	0.37	0.42	16.4	-	0.037	35

© 2002 ISIJ

30 scanning electron microscope permitted the automatic micro-texture analysis by the on-line interpretation of the electron back-scattered diffraction (EBSD) patterns. Texture measurements were also made with an automated pole figure goniometer using MoKα radiation. The X-ray diffraction data were obtained on the mid-thickness sections of the ND plane. Orientation distribution function (ODF) was obtained from (110), (200), and (211) three pole figures. For the evaluation of the degree of ridging, uniaxial tensile tests were performed at a strain rate of 10 mm/min and interrupted at a strain of 0.15. The surface roughness due to ridging was measured using a Surftest 501 (Series 178) manufactured by Mitutoyo surface measuring instrument.

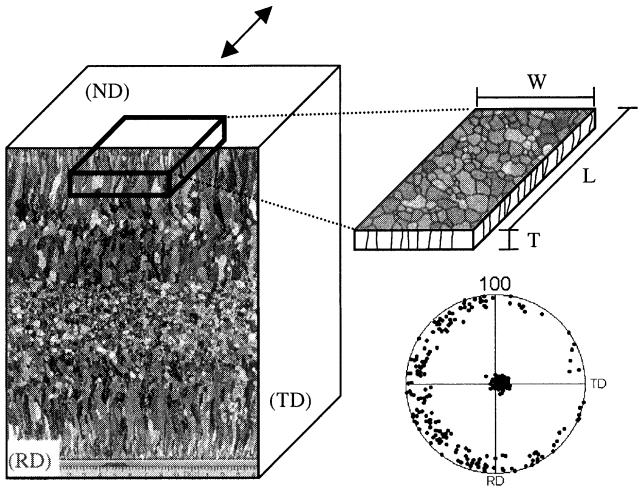

Fig. 1. Schematic shape of the steel specimens and the observed microstructure of continuously cast slab.

Table 2. Annealing conditions.

Annealing process	409L	430
Hot band	930°C, 1 min	850°C, 5 hr
Cold rolled sheet	930°C, 30 sec	860°C, 30 sec

3. Results

Figure 2 shows the microstructural variation observed on the mid-thickness of ND plane at each process stage of 409L and 430 steels. In 409L steel, the initial columnar structure was elongated upon rolling. The initial columnar structure was found to be remained in a band shape in HRA and CRA conditions (Figs. 2(b) and 2(c)). However, in the case of 430 steel, the band structure originated from the initial columnar structure was reduced significantly, as shown in Fig. 2(f), due to the existence of austenitic phase in the hot rolling stage.

Texture evolution of the two steels was also examined at each process stage. **Figure 3** shows the variation of fibre intensities measured on the ND plane of central layer depending on process stage of 409L and 430 steels. The difference in fibre intensities was pronounced in α-fibre between the two steels, while that of γ-fibre was negligible. The α-fibre intensities of 409L steel were found greater in both HRA and CRA condition than those of 430 steel. The α-fibre intensities measured at the CRA condition were relatively low in comparison to those measured at the HRA condition in both steels.

Figure 4 exhibits the crystal orientation maps obtained from TD plane of HRA specimens. The orientation of each grain was represented as red, green and blue colors corresponding to 001, 110 and 111 poles, respectively, as shown in the standard stereograph. The orientation of the elongated grains obtained at the central layer of both steels was identified as $\{001\}\langle 110\rangle$. The 409L steel exhibited only a few elongated coarse grains in HRA condition. In 430

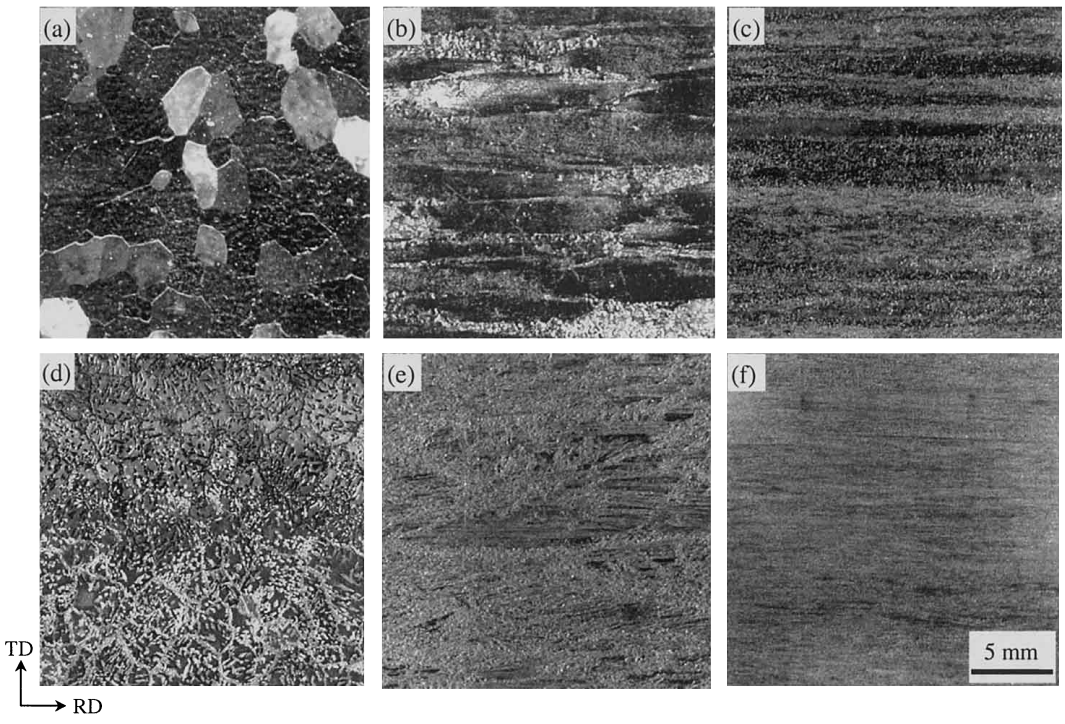

Fig. 2. Microstructural variation observed on the mid-thickness of ND plane at each process stage of 409L (a to c) and 430 (d to f)steels: (a), (d) slab; (b), (e) HRA; and (c), (f) CRA.

© 2002 ISIJ

steel, however, the elongation was revealed as a significant amount of grain colonies or grains clusters.

Figure 5 shows three dimensional microstructures obtained from the CRA specimens. The large grain shown in Fig. 5 corresponded to the coarse band structure, as already shown in Fig. 2. The size of the large grain in 409L steel was greater than that of 430 steel.

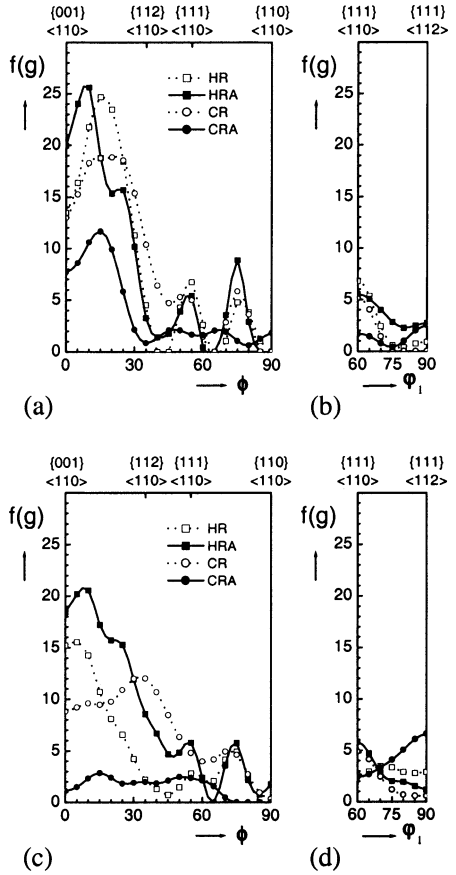

Fig. 3. Variation of fibre intensities measured on the ND plane of central layer depending on process stage of 409L (a and b) and 430 (c and d) steels: (a), (c) α-fibre; (b), (d) γ-fibre.

The existence of grain colonies was also examined by using OIM. **Figure 6** exhibits the crystal orientation maps with a (110) pole obtained on the ND, RD, and TD planes in CRA condition. In order to identify the presence of grain colonies, the EBSD analyses were confined to the region of band structure, as already shown in Fig. 2. Grain colonies with three different orientations were clearly found: $\{112\}\langle 110\rangle$, $\{001\}\langle 110\rangle$, and $\{001\}\langle 100\rangle$ orientations. The orientations could be highlighted with a 15 degree tolerance in Fig. 6. The $\{001\}\langle 110\rangle$ and $\{112\}\langle 110\rangle$ orientations were the major orientations. Only the former orientation was hypothesized in the theoretical models.[1,3]

In the present study, micro-texture measurements were conducted mostly on the mid-thickness of ND plane, because it was on the ND plane among each section that the existence of grain colonies was easily identified. In **Fig. 7**, the highlighted crystal orientation maps were overlapped with elongated band structure observed in CRA condition. The well-defined periodic arrays of bands of grain colonies were found along the band structure. Figure 7(a) clearly revealed that the coarse band structure (bright gray colored) formed in CRA condition of 409L steel was composed of grain-colonies having $\{001\}\langle 110\rangle$ and $\{112\}\langle 110\rangle$ orientations. Within the grain consisting of grain colony, significant amounts of low angle boundaries were also found, as shown in Fig. 7(c). In 430 steel, however, the fine band structure consisted of fine colonies with the same orientation.

4. Discussion

4.1. Origin of Grain Colonies

While there is little doubt that ridging is resulted from anisotropic plastic flow of mixed textures, the understanding of detailed mechanism is still in debate due to the lack of direct evidence for the existence of grain colonies, which has been a hypothesis for the theoretical model proposed.[1–3] In addition, the evolution of specific texture

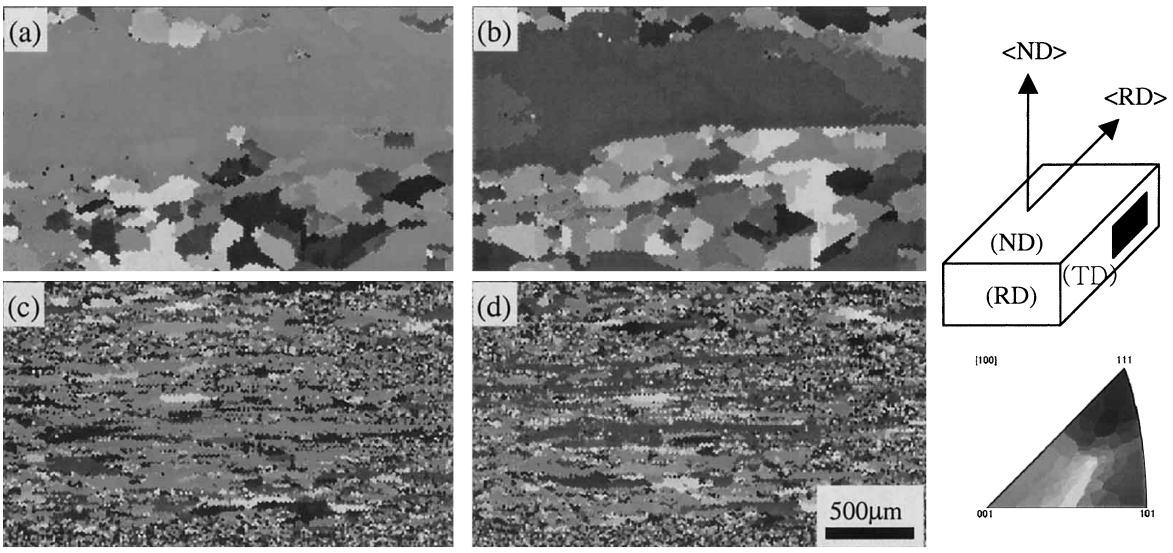

Fig. 4. Crystal orientation map obtained from TD plane of HRA specimens: (a) ⟨ND⟩ orientation of grains in 409L steel; (b) ⟨RD⟩ orientation of grains in 409L steel; (c) ⟨ND⟩ orientation of grains in 430 steel; (d) ⟨RD⟩ orientation of 430 steel.

© 2002 ISIJ

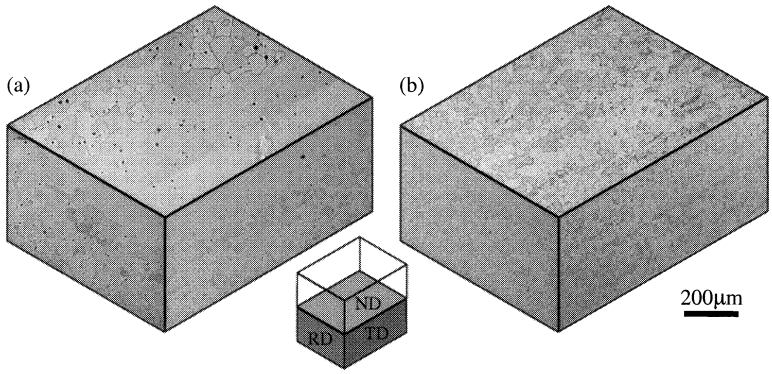

Fig. 5. Three dimensional microstructure observed in CRA specimens of type 409L(a) and type 430(b) steels.

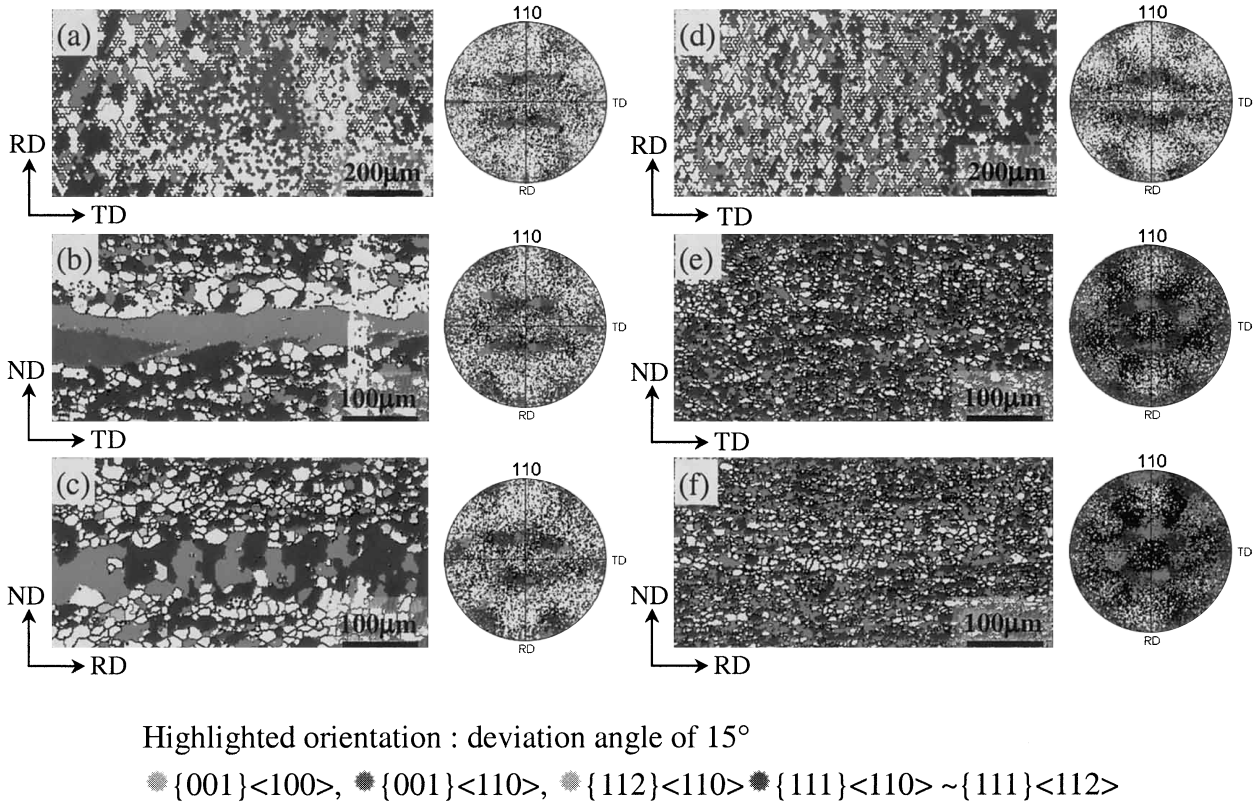

Fig. 6. Crystal orientation map with (110) pole figure observed on each plane of 409L (a to c) and 430 (d to f) steels in CRA condition: (a), (d) ND plane; (b), (e) RD plane; (c), (f) TD plane.

associated with grain colonies has not been understood well. In the present study, the grain colonies having both {001}⟨110⟩ and {112}⟨110⟩ orientations was clearly observed as shown in Figs. 6 and 7. The origin of these orientations depends on both crystal rotation toward stable orientation during rolling and recrystallization behavior.

The EBSD results shown in Figs. 6 and 7 indicated that the band structure associated with grain colonies or clusters were mostly observed in the mid-thickness region of the specimen. The results seems to be caused by stable orientation components for bcc alloy under plane strain condition such as rolling deformation.[9] While the surface regions are deformed mainly by shear strain due to a large friction between roll and steel strip during hot rolling, the mid-thickness regions are deformed mainly by plane strain. Therefore, pronounced texture gradients along the thickness could be easily formed in hot band, such as {001}⟨110⟩ and {112}⟨110⟩ orientations at the central region and the Goss orientation developed at surface region.[10–12] It is, thus, reasonable to estimate that the {001}⟨110⟩ and {112}⟨110⟩ orientations observed at the central region is still remained during cold rolling as stable orientation components. In addition, the texture evolution is also dependent on the degree of crystal rotation during rolling. The texture formation from initial {001}⟨*uvw*⟩ orientation of columnar cast structure to the {001}⟨110⟩ and {112}⟨110⟩ orientations was pronounced due to easy crystal rotation toward stable orientation during rolling.[13]

The ferritic stainless steels are hard to be recrystallized during hot rolling because of very fast dynamic recovery. It has been reported that the recrystallization rate is extremely low in the {001}⟨110⟩ and {112}⟨110⟩ crystals.[14–17] The

© 2002 ISIJ

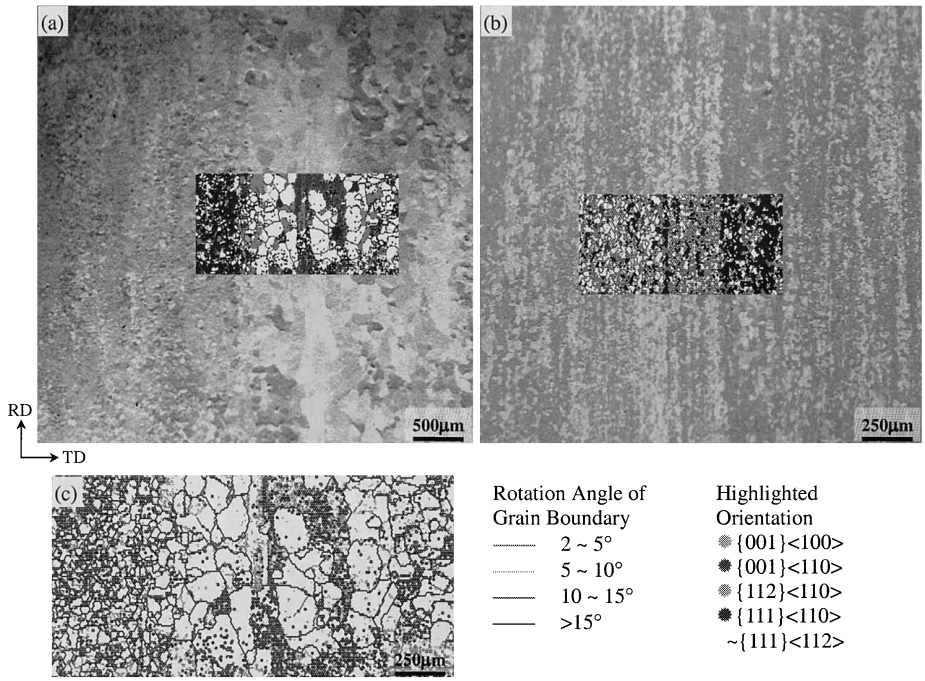

Fig. 7. Crystal orientation map overlapped with band structure observed on the mid-thickness of ND plane in CRA specimens of (a) 409L steel, (b) 430 steel. Low angle grain boundaries were observed within grain colonies of 409L steel (c).

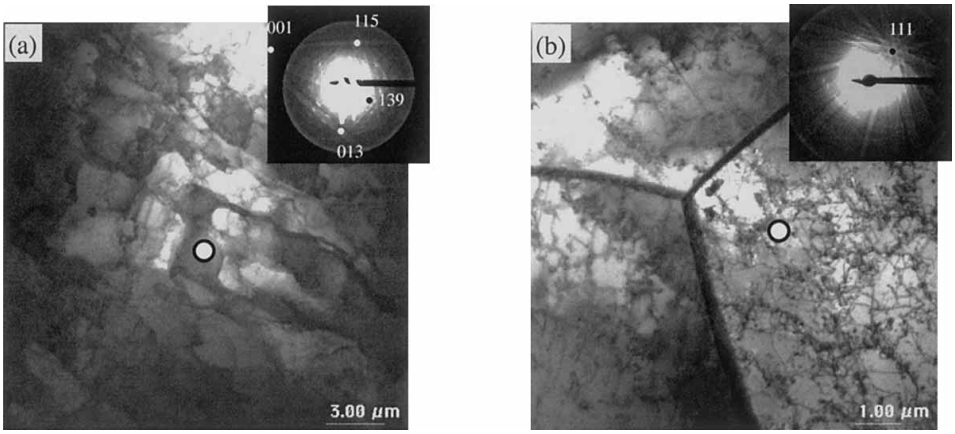

Fig. 8. TEM micrographs obtained on the mid-thickness region of CRA specimen in 409L steel: (a) cell structure observed in the grain having near [001]//ND orientation; (b) high angle grain boundaries as a results of recrystallization in the grain having near [111]//ND orientation.

deformation texture, mostly α-fibre texture with $\{hkl\}\langle 110\rangle$ orientation, thus, can be retained easily in the mid-thickness of hot band (HR specimen). The strong α-fiber texture found in the hot band did not change significantly upon annealing, as shown in Fig. 3. At a CRA condition, the band structures having $\{001\}\langle 110\rangle$ and $\{112\}\langle 110\rangle$ orientations were still remained, as shown in Fig. 7, although the intensity of α-fiber observed by ODF analysis decreased considerably, as shown in Fig. 3. Coarse grains within grain colonies revealed large amount of low angle grain boundaries represented by green colored, as shown in Fig. 7(c). The results suggest an active recovery without recrystallization upon annealing after cold rolling. In order to confirm whether the grain colonies recrystallize or not upon annealing, TEM observation was performed for 409L steel. Cell structures were found within a coarse grain located inside the grain colonies, as shown in **Fig. 8**(a). The large amount of cell boundaries was derived from the recovery without recrystallization during annealing. The microstructure is quite comparable with the recrystallized microstructure shown in Fig. 8(b). The kikuchi pattern analysis revealed the orientation of the grain colonies as near [001]//ND confirming the results obtained from the EBSD analyses (Fig. 7). Consequently, the presence of grain colonies having the $\{001\}\langle 110\rangle$ and $\{112\}\langle 110\rangle$ orientations found at finally annealed (CRA) sheet is caused by both the suppressed recrystallization and crystal rotation toward the α-fibre texture, which is the one of the stable texture components upon rolling deformation.

4.2. Grain Colonies and Ridging Phenomena

The macroscopic appearance of ridging was easily found

© 2002 ISIJ

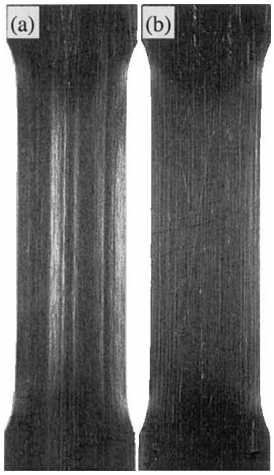

Fig. 9. Macroscopic appearance of ridging found on the tensile specimens: (a) 409L steel (ridging height: 55 μm); (b) 430 steel (ridging height : 23 μm).

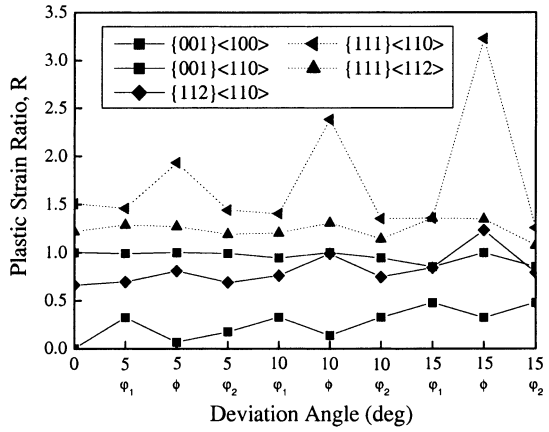

Fig. 10. Variation of plastic strain ratio (R_0-value) depending on the deviation angle for each ideal orientations.

on the tensile specimens, as shown in **Fig. 9**. The ridging characteristics were different between 409L and 430 steels. The ridging height of 409L steel was 2.5 times higher than that of 430 steel at the same tensile elongation (15%). Both amplitude and wavelength of corrugations in 430 steel were relatively smaller and uniform compared to those of 409L steel. The shape of these corrugations was quite compatible with the size and distribution of grain colonies as already observed in Figs. 2 and 7. The difference in ridging appearance directly resulted from the difference in the size and distribution of grain colonies having $\{001\}\langle 110\rangle$ and $\{112\}\langle 110\rangle$ orientations.

It is well known that plastic strain ratio (*R*-value) depends on the crystal orientation, and that the *R*-value for each ideal orientation can be calculated.[18,19] The variation of plastic strain ratio (*R*-value) depending on the deviation angle for each ideal orientation could be calculated, as shown in **Fig. 10**. The *R*-value for $\{001\}\langle 100\rangle$, $\{001\}\langle 110\rangle$, and $\{112\}\langle 110\rangle$ orientations was relatively low compared to that of $\{111\}\langle uvw\rangle$ orientation. It is, thus, obvious that the presence of grain colonies can cause different *R*-value compared to matrix, which consequently cause the occurrence of ridging. The current results may support Chao[1] and Wright[3]'s ridging mechanisms among the previously proposed models.[1–3,6–8]

5. Conclusions

(1) The grain colonies or grain clusters were found to have mainly $\{001\}\langle 110\rangle$ and $\{112\}\langle 110\rangle$ orientations, located at the mid-thickness region of sheet samples of the model alloy systems.

(2) The difference in the ridging characteristics between 409L and 430 steel mainly derives from the difference in the size and distribution of grain colonies having $\{001\}\langle 110\rangle$ and $\{112\}\langle 110\rangle$ orientations.

(3) The existence of grain colonies with the $\{001\}\langle 110\rangle$ and $\{112\}\langle 110\rangle$ orientations is caused by both the suppressed recrystallization and crystal rotation toward the α-fibre texture, which is the one of the stable texture components upon rolling deformation.

REFERENCES

1) H. C. Chao: *Trans. Am. Soc. Met*., **60** (1967), 37.
2) H. Takechi, H. Kato, T. Sunami and T. Kakayama: *J. Jpn. Inst. Met*., **31** (1967), 717.
3) R. N. Wright: *Metall. Trans*., **3** (1972), 83.
4) J. Venables and C. Harland: *Philos. Mag*., **27** (1973), 1193.
5) V. Randle: Microtexture Determination and its Applications, Inst. of Materials, London, (1992).
6) N. J. Wittridge and R. D. Knutsen: Thermo-Mechanical Processing in Theory, Modelling & Practice, Swedish Society for Materials Technology, Stockholm, (1997), 390.
7) K. Bethke, M. Holscher and K. Lucke: *Mater. Sci. Forum*, **157**–**162** (1994), 1137.
8) M. Brochu, T. Yokota and S. Satoh: *ISIJ Int*., **37** (1997), 872.
9) T. Taoka, E. Furubayashi and S. Takeuchi: *Trans. Iron Steel Inst. Jpn*., **6** (1966), 290.
10) M. Holscher, D. Raabe and K. Lucke: *Steel Res*., **62** (1991), 567.
11) D. Raabe and K. Lucke: *Mater. Sci. Technol*., **9** (1993), 302.
12) S. Y. Cho, H. C. Kim and M. Y. Huh: *J. Korean Inst. Met. & Mater*., **38** (2000), 963.
13) S. H. Park, K. Y. Kim, Y. D. Lee and C. G. Park: Proc. ICOTOM 12, NRC Research Press, Ottawa, (1999), 1095.
14) W. R. Hibbard, Jr. and W. R. Tully: *Trans. Metall. Soc. AIME*, **221** (1961), 336.
15) T. Taoka, E. Furubayashi and S. Takeuchi: *Trans. Iron Steel Inst. Jpn*., **7** (1967), 95.
16) T. Wada, F. Matsumoto and K. Kuroki: *J. Jpn. Inst. Met*., **32** (1968), 767.
17) N. Tsuji, K. Tsuzaki and T. Maki: *ISIJ Int*., **33** (1993), 783.
18) R. K. Ray, J. J. Jonas and R. E. Hook: *Int. Mater. Rev*., **39** (1994), 129.
19) H.-T. Jeong and D. N. Lee: *J. Korean Inst. Met. & Mater*., **35** (1997), 550.

© 2002 ISIJ